A single-photon transistor using nanoscale surface plasmons

DARRICK E. CHANG[1], ANDERS S. SØRENSEN[2], EUGENE A. DEMLER[1] AND MIKHAIL D. LUKIN[1]*

[1]Physics Department, Harvard University, Cambridge, Massachusetts 02138, USA
[2]QUANTOP, Danish Quantum Optics Center and Niels Bohr Institute, DK-2100 Copenhagen Ø, Denmark
*e-mail: lukin@physics.harvard.edu

Photons rarely interact—which makes it challenging to build all-optical devices in which one light signal controls another. Even in nonlinear optical media, in which two beams can interact because of their influence on the medium's refractive index, this interaction is weak at low light levels. Here, we propose a novel approach to realizing strong nonlinear interactions at the single-photon level, by exploiting the strong coupling between individual optical emitters and propagating surface plasmons confined to a conducting nanowire. We show that this system can act as a nonlinear two-photon switch for incident photons propagating along the nanowire, which can be coherently controlled using conventional quantum-optical techniques. Furthermore, we discuss how the interaction can be tailored to create a single-photon transistor, where the presence (or absence) of a single incident photon in a 'gate' field is sufficient to allow (or prevent) the propagation of subsequent 'signal' photons along the wire.

In analogy with the electronic transistor, a photonic transistor is a device where a small optical 'gate' field is used to control the propagation of another optical 'signal' field via a nonlinear optical interaction[1,2]. Its fundamental limit is the single-photon transistor, where the propagation of the signal field is controlled by the presence or absence of a single photon in the gate field. Such a nonlinear device has many interesting applications from optical communication and computation[2] to quantum-information processing[3]. However, its practical realization is challenging because the requisite single-photon nonlinearities are generally very weak[1]. Several schemes for producing nonlinearities at the single-photon level are currently being explored, ranging from resonantly enhanced nonlinearities of atomic ensembles[4–8] to individual atoms coupled to photons in cavity quantum electrodynamics (QED)[9–13], and possibilities of single-photon switching in these contexts have also been proposed[5,14]. However, a robust, practical approach has yet to emerge.

Recently, a new method to achieve strong coupling between light and matter was proposed[15]. It makes use of the tight concentration of optical fields associated with guided surface plasmons on conducting nanowires to achieve strong interaction with individual optical emitters. The tight localization of these fields causes the nanowire to act as a very efficient lens that directs the majority of spontaneously emitted light into the surface-plasmon modes, resulting in efficient generation of single surface plasmons (that is, single photons)[15]. Here, we show that such a system enables the realization of remarkable nonlinear optical phenomena, where individual photons strongly interact with each other. As an example, we describe how this nonlinearity may be exploited to implement a single-photon transistor. Although ideas for developing plasmonic analogues of electronic devices by combining surface plasmons with electronics are already being explored[16,17], the process we describe here opens up fundamentally new possibilities, in that it combines the ideas of plasmonics with the tools of quantum optics[5,7,8,10] to achieve unprecedented control over the interactions of individual light quanta.

NANOWIRE SURFACE PLASMONS: INTERACTION WITH MATTER

Surface plasmons are propagating electromagnetic modes confined to the surface of a conductor–dielectric interface[16,18]. Their unique properties make it possible to confine them to subwavelength dimensions, which has led to fascinating new approaches to waveguiding below the diffraction limit[19], enhanced transmission through subwavelength apertures[20], subwavelength imaging[21,22] and enhanced fluorescence[23–25]. Recently, signatures of strong coupling between molecules and surface plasmons have also been observed via a splitting of the surface-plasmon mode dispersion[26,27]. It is important to emphasize that these observations can be described in terms of classical, linear optical effects. Below, however, we consider how the confinement of surface plasmons on a conducting nanowire and their coupling to an individual, proximal optical emitter (see Fig. 1a,b) can also give rise to controllable nonlinear interactions between single photons.

Much like a single-mode fibre, the surface-plasmon modes of a conducting nanowire constitute a one-dimensional single-mode continuum that can be indexed by the wavevectors k along the direction of propagation[15,19,28]. Unlike a fibre[29], however, the nanowire exhibits good confinement and guiding even when its radius is reduced well below the optical wavelength ($R \ll \lambda_0$). Specifically, in this limit, the surface plasmons exhibit strongly reduced wavelengths and small transverse-mode areas relative to free-space radiation, which scale as $\lambda_{pl} \propto 1/k \propto R$ and $A_{eff} \propto R^2$, respectively. The tight confinement results in a large coupling constant $g \propto 1/\sqrt{A_{eff}}$ between the surface-plasmon modes and any proximal emitter with a dipole-allowed transition. The reduction in group velocity also yields an enhancement of the density of states, $D(\omega) \propto 1/R$. The spontaneous emission rate into the surface plasmons, $\Gamma_{pl} \sim g^2(\omega)D(\omega) \propto (\lambda_0/R)^3$, can therefore be much larger than the emission rate Γ' into all other possible channels. Physically, Γ' includes contributions both from emission into free space and non-radiative emission via ohmic losses in the conductor[15]. A relevant figure of merit is an effective Purcell
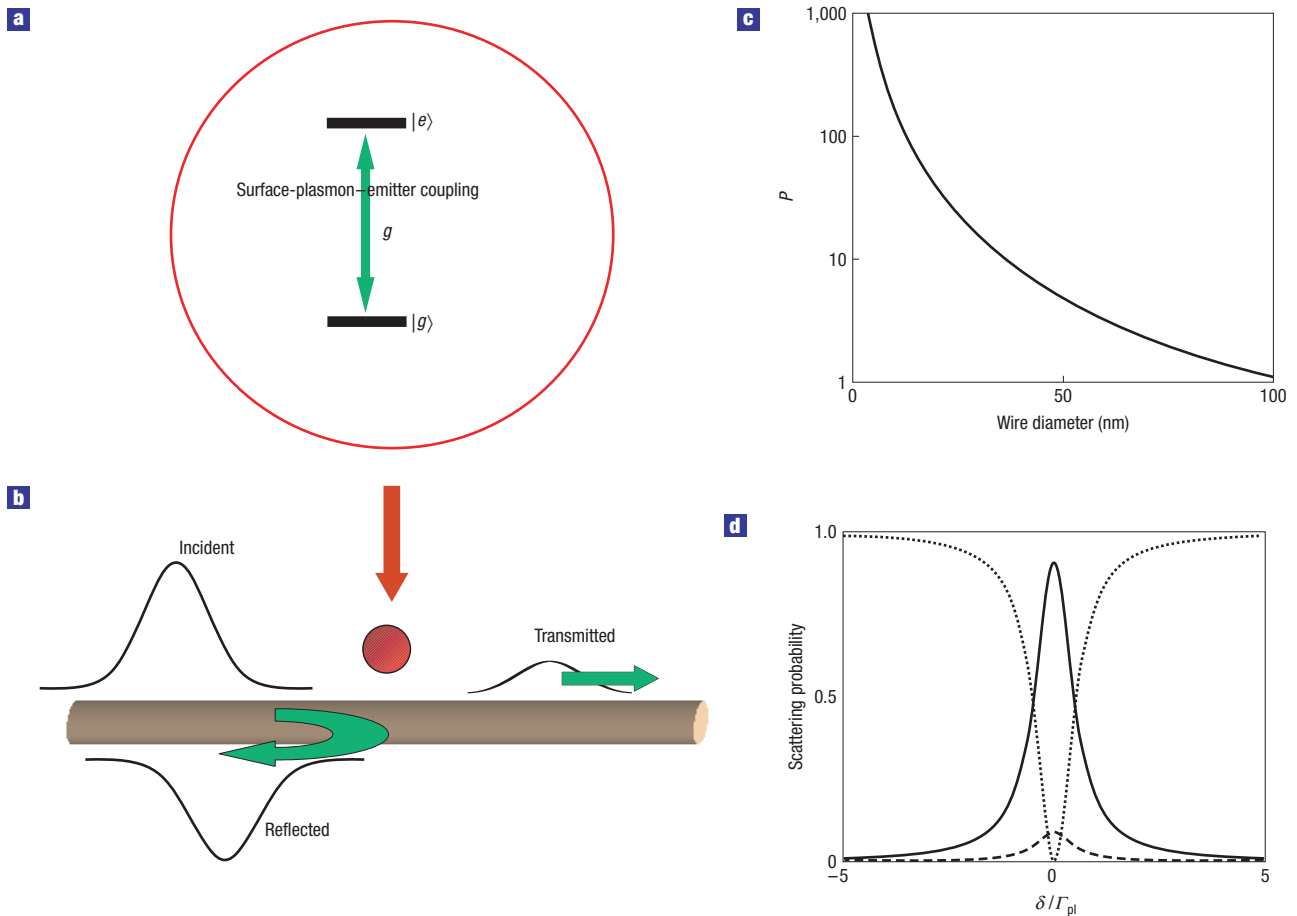
Figure 1 Interaction of single surface plasmons with a single emitter. a, Two-level emitter interacting with the nanowire. States $|g\rangle$ and $|e\rangle$ are coupled via the surface-plasmon modes with a strength g. **b**, Schematic diagram of a single incident photon scattered off a near-resonant emitter. The interaction leads to reflected and transmitted fields whose amplitudes can be calculated exactly. **c**, The maximum Purcell factor of an emitter positioned near a silver nanowire ($\epsilon \approx -50 + 0.6i$) and surrounded by a uniform dielectric ($\epsilon = 2$), as a function of wire diameter. The plot is calculated using the method in refs 15,28 and the silver properties used correspond to a free-space wavelength of $\lambda_0 = 1\,\mu\mathrm{m}$. **d**, Probabilities of reflection (solid line), transmission (dotted line) and loss (dashed line) for a single photon incident on a single emitter, as a function of detuning. The Purcell factor for this system is taken to be $P = 20$.

factor, $P \equiv \Gamma_{\mathrm{pl}}/\Gamma'$, which can exceed 10^3 in realistic systems (see Fig. 1c). This result is in contrast with nanoscale optical fibres, where the inability to confine photons below the diffraction limit results in values of $P \lesssim 1$ (ref. 30). Furthermore, we note that this strong coupling is broadband, as it arises purely from geometrical considerations as opposed to any resonant features of the surface plasmons. This is in direct contrast, for example, to the mechanism by which strong coupling is achieved in cavity QED.

Motivated by these considerations, we now describe a general one-dimensional model of an emitter strongly coupled to a set of travelling electromagnetic modes (see Fig. 1a,b). We first consider a simple two-level configuration for the emitter, consisting of ground and excited states ($|g\rangle$, $|e\rangle$) separated by frequency ω_{eg}. The corresponding hamiltonian is

$$H = \hbar(\omega_{\mathrm{eg}} - i\Gamma'/2)\sigma_{ee} + \int \mathrm{d}k\,\hbar c|k|\hat{a}_k^\dagger \hat{a}_k$$
$$- \hbar g \int \mathrm{d}k\,(\sigma_{eg}\hat{a}_k e^{ikz_a} + \mathrm{h.c.}), \qquad (1)$$

where $\sigma_{ij} = |i\rangle\langle j|$, $\hat{a}_k$ is the annihilation operator for the mode with wavevector k and z_a is the emitter position. We have assumed that a linear dispersion relation holds over the relevant frequency range, $\nu_k = c|k|$, where c is the group velocity of the surface plasmons, and similarly that g is frequency-independent. In the spirit of the 'quantum jump' description of an open system[31], we have also included a non-Hermitian term in H due to the decay of state $|e\rangle$ at a rate Γ' into the other channels. This effective hamiltonian accurately describes the dynamics provided that the thermal energy $k_B T \ll \hbar\omega_{\mathrm{eg}}$, where k_B is the Boltzmann constant (see the Supplementary Information for further discussion of this model).

SINGLE EMITTER AS A SATURABLE MIRROR

The propagation of surface plasmons can be markedly altered by interaction with the single two-level emitter. In particular, for low incident powers, the interaction occurs with near-unit probability, and each photon can be reflected with very high efficiency. However, for higher powers the emitter response rapidly saturates, as it is not able to scatter more than one photon at a time.
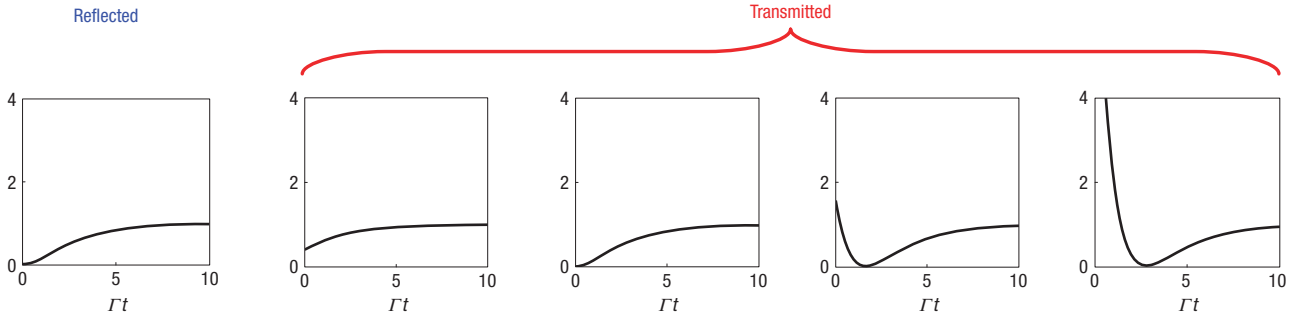
Figure 2 Second-order correlation function $g^{(2)}(t)$ for the reflected and transmitted fields at low incident power ($\Omega_c/\Gamma = 0.01$). $g^{(2)}(t)$ for the reflected field is independent of P at low powers. For the transmitted field, going from left to right, the Purcell factors are $P = 0.6, 1, 1.5$ and 2, respectively. A rise in $g^{(2)}(0)$ for large Purcell factors indicates a strong initial bunching of photons at the transmitted end. This initial bunching is accompanied by an antibunching effect, $g^{(2)}(t_0) \approx 0$, at some later time $t_0 = (4 \log P)/\Gamma$ for $P \geq 1$. For high incident powers (not shown), $g^{(2)}(t)$ approaches unity for all times owing to a saturation of the atomic response.

The low-power behaviour can be understood by first considering the scattering of a single photon, as shown schematically in Fig. 1b. As we are interested only in surface-plasmon modes near the optical frequency ω_{eg}, we can effectively treat left- and right-propagating surface plasmons as completely separate fields. We define operators that annihilate a left (right)-propagating photon at position z, $\hat{E}_{L(R)}(z) = (1/\sqrt{2\pi}) \int dk \, e^{ikz} \hat{a}_{L(R),k}$, where operators acting on the left and right branches are assumed to have vanishing commutation relations with the other branch. An exact solution to the scattering from the right to left branches in the limit $P \rightarrow \infty$ was derived in ref. 32 by solving for the scattering eigenstates of the system, and the approach can be generalized to finite P (see the Methods section). The reflection coefficient for an incoming photon of wavevector k is

$$r(\delta_k) = -\frac{1}{1 + \Gamma'/\Gamma_{pl} - 2i\delta_k/\Gamma_{pl}}, \qquad (2)$$

where $\delta_k \equiv ck - \omega_{eg}$ is the photon detuning, whereas the transmission coefficient is given by $t(\delta_k) = 1 + r(\delta_k)$. Here, $\Gamma_{pl} = 4\pi g^2/c$ is the decay rate into the surface plasmons, as obtained by application of Fermi's golden rule to the hamiltonian in equation (1). On resonance, $r \approx -(1 - 1/P)$, and thus for large Purcell factors the emitter in state $|g\rangle$ acts as a nearly perfect mirror, which simultaneously imparts a π-phase shift on reflection. The bandwidth $\Delta\omega$ of this process is determined by the total spontaneous emission rate, $\Gamma = \Gamma_{pl} + \Gamma'$, which can be quite large. Furthermore, the probability κ of losing the photon to the environment is strongly suppressed, $\kappa \equiv 1 - \mathcal{R} - \mathcal{T} = 2\mathcal{R}/P$, where $\mathcal{R}(\mathcal{T}) \equiv |r|^2 (|t|^2)$ is the reflectance (transmittance). These results are shown in Fig. 1d, where $\mathcal{R}, \mathcal{T}$ and κ are plotted as a function of detuning δ_k, taking a conservative value of $P = 20$.

The nonlinear response of the system can be seen by considering the interaction of a single emitter not just with a single photon, but with multiphoton input states. To be specific, we consider the case when the incident field consists of a coherent state, the quantum-mechanical state that most closely corresponds to a classical field[31] (note also similar work in refs 33,34 where scattering of two-photon states is considered). We assume that the incident field propagates to the right, with $\langle \hat{E}_R \rangle = \mathcal{E}_c(z, t)$, and that the emitter is initially in the ground state. As shown in the Methods section, by transformation the initial coherent state can be formally mapped to an external Rabi frequency (given by $\Omega_c = \sqrt{2\pi} g \mathcal{E}_c$) in the hamiltonian, which allows all quantities of interest (for example, field correlation functions) to be calculated

exactly. For a narrow bandwidth ($\delta\omega \ll \Gamma$), resonant ($\delta_k = 0$) input field, the steady-state transmittance and reflectance are found to be

$$\mathcal{T} = \frac{1 + 8(1+P)^2(\Omega_c/\Gamma)^2}{(1+P)^2(1 + 8(\Omega_c/\Gamma)^2)},$$

$$\mathcal{R} = \left(1 + \frac{1}{P}\right)^{-2} \frac{1}{1 + 8(\Omega_c/\Gamma)^2}.$$

At low powers ($\Omega_c/\Gamma \ll 1$), the emitter has scattering properties identical to the single-photon case, $\mathcal{R} \approx (1 + 1/P)^{-2}$, $\mathcal{T} \approx (1+P)^{-2}$, and for large Purcell factors the single emitter again acts as a perfect mirror. At high incident powers ($\Omega_c/\Gamma \gg 1$), however, the emitter saturates and most of the incoming photons are transmitted past with no effect, $\mathcal{T} \rightarrow 1$, $\mathcal{R} \sim \mathcal{O}((\Gamma/\Omega_c)^2)$. The significance of these results can be understood by noting that saturation is achieved at a Rabi frequency $\Omega_c \sim \Gamma$ that, in the limit of large P, corresponds to a switching energy of a single quantum ($\sim \hbar\nu$) within a pulse of duration $\sim 1/\Gamma$.

PHOTON CORRELATIONS

The strongly nonlinear atomic response at the single-photon level leads to pronounced modification of photon statistics that cannot be captured by only considering average intensities, but appear in higher-order correlations of the transmitted and reflected fields. Specifically, we focus on the normalized second-order correlation functions, $g_{R,L}^{(2)}(t)$, which for a stationary process are defined as

$$g_{\beta=R,L}^{(2)}(z,t) \equiv \langle \hat{E}_\beta^\dagger(z,\tau) \hat{E}_\beta^\dagger(z, \tau+t) \hat{E}_\beta(z, \tau+t) \hat{E}_\beta(z, \tau) \rangle / \langle \hat{E}_\beta^\dagger(z,\tau) \hat{E}_\beta(z,\tau) \rangle^2,$$

where t denotes the difference between the two observation times τ and $\tau + t$.

The statistics of the reflected field is identical to the well-known result for resonance fluorescence[31] in three dimensions (see Fig. 2) because it is a purely scattered field. It follows that the field is strongly antibunched, $g^{(2)}(0) = 0$, as the emitter can only absorb and re-emit one photon at a time. The transmitted field, however, has unique properties because it is a sum of the incident and scattered fields. For near-resonant excitation and low powers (see the Methods section),

$$g^{(2)}(t) = e^{-\Gamma t}\left(P^2 - e^{\Gamma t/2}\right)^2 + \mathcal{O}(\Omega_c^2/\Gamma^2),$$
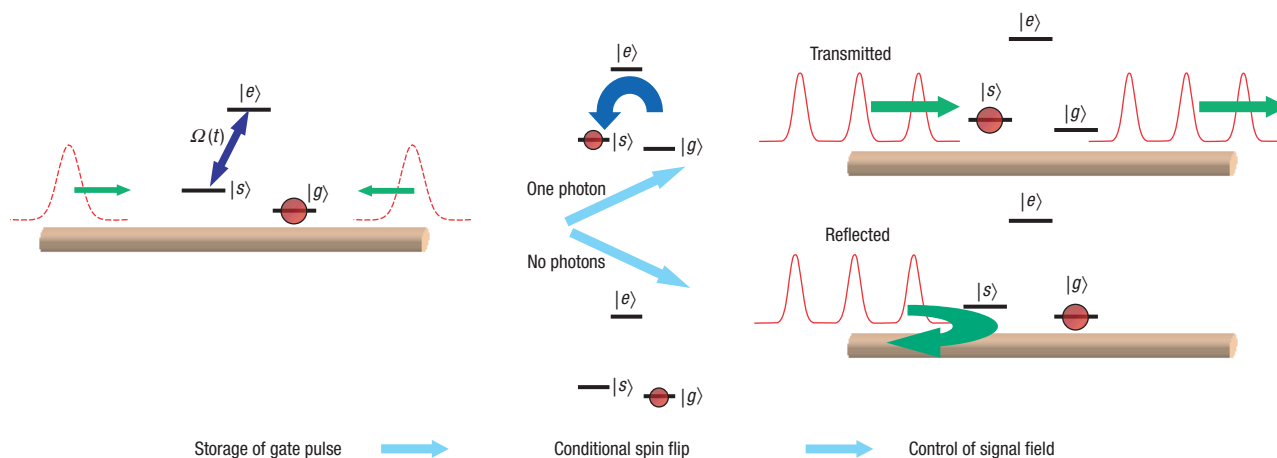
809

Figure 3 Schematic diagram of transistor operation involving a three-level emitter. In the storage step, a gate pulse consisting of zero or one photon is split equally in counter-propagating directions and coherently stored using an impedance-matched control field $\Omega(t)$. The storage results in a spin flip conditioned on the photon number. A subsequent incident signal field is either transmitted or reflected depending on the photon number of the gate pulse, owing to the sensitivity of the propagation to the internal state of the emitter.

whereas for high powers, $g^{(2)}(t)$ approaches unity for all times owing to saturation of the atomic response. The low-power behaviour reflects that of an efficient single-photon switch. Specifically, for $P \gg 1$, individual photons have a large reflection probability, but when two photons are incident simultaneously the transition saturates, so that pairs have a much larger probability of transmission (for $P \ll 1$, the emitter has little influence and the transmitted statistics are almost unchanged). This phenomenon yields a strong bunching effect at $t = 0$ that behaves like $g^{(2)}(0) \approx P^4$. Furthermore, at time $t_0 = (4 \log P)/\Gamma$ there is a subsequent antibunching and perfect vanishing of $g^{(2)}(t)$ for weak input fields. A more detailed analysis of these features is given in the Supplementary Information (also see ref. 35 for a discussion of a similar phenomenon in cavity QED).

IDEAL SINGLE-PHOTON TRANSISTOR

A greater degree of coherent control over the field interaction can be gained by considering a multilevel emitter, such as the three-level configuration shown in Fig. 3. Here, a metastable state $|s\rangle$ is decoupled from the surface plasmons owing to, for example, a different orientation of its associated dipole moment, but is resonantly coupled to $|e\rangle$ via some classical, optical control field with Rabi frequency $\Omega(t)$. States $|g\rangle$ and $|e\rangle$ remain coupled via the surface-plasmon modes as discussed earlier. Using this system, we now describe a process in which a single 'gate' photon can completely control the propagation of subsequent 'signal' pulses consisting of either individual or multiple photons, whose timing can be arbitrary. In analogy to the electronic counterpart, this corresponds to an ideal single-photon transistor.

We first describe how one can achieve coherent storage of a single photon, which is an important ingredient as it provides an atomic memory of the gate field and thus allows the gate to interact with the subsequent signal. We initialize the emitter in $|g\rangle$ and apply the control field $\Omega(t)$ simultaneous with the arrival of a single photon in the surface-plasmon modes. The control field, if properly chosen (or 'impedance-matched')[36], will result in capture of the incoming single photon while inducing a spin flip from $|g\rangle$ to $|s\rangle$. Generally, by time-reversal symmetry[37], the optimal storage strategy is the time-reversed process of single-photon generation,

where the emitter is driven from $|s\rangle$ to $|g\rangle$ by the external field while emitting a single photon whose wavepacket depends on $\Omega(t)$. By this argument, it is evident that optimal storage is obtained by splitting the incoming pulse and having it incident from both sides of the emitter simultaneously (see Fig. 3), and that there is a one-to-one correspondence between the incoming pulse shape and the optimal field $\Omega(t)$. The storage efficiency is identical to that of single-photon generation and is thus given by $\sim 1 - 1/P$ for large P (ref. 15) (also see the Supplementary Information for an exact solution of the system dynamics). A detailed analysis reveals that this optimum is achievable for any input pulse of duration $T \gg 1/\Gamma$ and for a certain class of pulses of duration $T \sim 1/\Gamma$ (ref. 37). Finally, if no photon impinges on the emitter, the pulse $\Omega(t)$ has no effect and the emitter remains in $|g\rangle$ for the entire process. The result is more generally described as a mapping between single surface-plasmon states and metastable atomic states $(\alpha|0\rangle + \beta|1\rangle)|g\rangle \rightarrow |0\rangle(\alpha|g\rangle + \beta|s\rangle)$.

Next, we consider the reflection properties of the emitter when the control field $\Omega(t)$ is turned off. If the emitter is in $|g\rangle$, the reflectance and transmittance derived above for the two-level emitter remain valid. On the other hand, if the emitter is in $|s\rangle$, any incident fields will simply be transmitted with no effect because $|s\rangle$ is decoupled from the surface plasmons. Therefore, with $\Omega(t)$ turned off, the three-level system effectively behaves as a conditional mirror whose properties depend sensitively on its internal state.

The techniques of state-dependent conditional reflection and single-photon storage can be combined to create a single-photon transistor, whose operation is shown in Fig. 3. The key principle is to use the presence or absence of a photon in an initial 'gate' pulse to conditionally flip the internal state of the emitter during the storage process, and to then use this conditional flip to control the flow of subsequent 'signal' photons arriving at the emitter. Specifically, we first initialize the emitter in $|g\rangle$ and apply the storage protocol for the gate pulse, which consists of either zero or one photon. The presence (absence) of a photon causes the emitter to flip to (remain in) state $|s\rangle$ ($|g\rangle$). Now, the interaction of each signal pulse arriving at the emitter depends on the internal state following storage. The storage and conditional spin flip causes the emitter to be either highly reflecting or completely transparent depending on the gate,
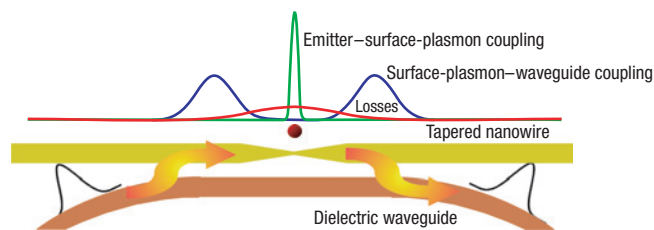
Figure 4 Schematic diagram of in- and out-coupling of surface plasmons on a tapered nanowire to an evanescently coupled low-loss dielectric waveguide. Here, a single photon originally in the waveguide is transferred to the nanowire, where it interacts with the emitter before being transferred back into the waveguide. The coupling between the nanowire and waveguide is efficient only when they are phase-matched (in the regions indicated by the blue peaks). The phase-matching condition is poor in the regions of the wire taper and in the bending region of the waveguide away from the nanowire. Dissipative losses (in red) are concentrated to a small region near the nanowire taper, owing to a large concentration of fields here.

and the system therefore acts as an efficient switch or transistor for the subsequent signal field.

The ideal operation of the transistor is limited only by the characteristic time over which an undesired spin flip can occur. In particular, if the emitter remains in $|g\rangle$ after storage of the gate pulse, the emitter can eventually be optically pumped to $|s\rangle$ on the arrival of a sufficiently large number of photons in the signal field. For strong coupling, the number of incident photons, n, that can be scattered before pumping occurs is given by the branching ratio of decay rates from $|e\rangle$ to these states, $n \sim \Gamma_{e \rightarrow g} / \Gamma_{e \rightarrow s}$, which can be large owing to the large decay rate $\Gamma_{e \rightarrow g} \geq \Gamma_{pl}$. Thus, $n \gtrsim P$ and the emitter can reflect $\mathcal{O}(P)$ photons before an undesired spin flip occurs. This number corresponds to the effective 'gain' of the single-photon transistor.

Finally, we note that there are other possible realizations of a single-photon transistor. The 'impedance-matching' condition and need to split a pulse for optimal storage, for example, can be relaxed using a small ensemble of emitters and photon storage techniques on the basis of electromagnetically induced transparency[38]. Here, storage also results in a spin flip within the ensemble that sensitively alters the propagation of subsequent photons.

INTEGRATED SYSTEMS

Inevitably, surface plasmons experience losses as they propagate along the nanowire, which could potentially limit their feasibility as long-distance carriers of information and in large-scale devices. For the nanowire, we must consider the trade-off between the larger Purcell factors obtainable with smaller diameters and a commensurate increase in dissipation due to the tighter field confinement. However, these limitations are not fundamental if we can integrate surface-plasmon devices with low-loss dielectric waveguides. Here, the surface plasmons can be used to achieve strong nonlinear interactions over very short distances, but are rapidly in- and out-coupled to conventional waveguides for long-distance transport. One such scheme is shown in Fig. 4, where excitations are transferred to and from the nanowire via an evanescently coupled, phase-matched dielectric waveguide. The losses will be small provided that the distance needed for the surface plasmons to be coupled in and out and interact with the emitter is smaller than the characteristic dissipation length, which can be accomplished using optimized surface-plasmon geometries (for example, tapered wires or nanotips[15,28]) or periodic structures

with engineered surface-plasmon dispersion relations[39]. Coupling efficiencies of ~95%, for example, are predicted using simple systems[28]. Such a conductor–dielectric interface would provide convenient integration with conventional optical elements, enable many nonlinear operations without loss and make large-scale integrated photonic devices feasible.

Another key feature of nanoscale surface plasmons is that the strong interaction is very robust. Because the large coupling occurs over a very large bandwidth and requires no special tuning of either the emitter or nanowire, surface plasmons are promising candidates for use with solid-state emitters such as quantum-dot nanocrystals[40] or colour centres[41], where the spectral properties can vary over individual emitters. Colour centres in diamond[41], for instance, are especially promising because they offer sharp optical lines and three-level internal configurations. At the same time, guided surface plasmons might be used for trapping isolated neutral atoms in the vicinity of suspended wires, thereby creating an effective interface for isolated atomic systems.

OUTLOOK

A single-photon transistor can be used for many important applications such as efficient single-photon detection, where the large gain in the signal field enables efficient detection of the gate pulse. This system also finds applications in quantum-information science. Schrodinger cat states of photons can be prepared, for example, if the gate pulse contains a superposition of zero and one photon, as this initial pulse becomes entangled with the propagation direction of potentially many subsequent signal photons. The controlled-phase gate for photons proposed in ref. 11 for cavity QED is also directly extendable to our system. In particular, this scheme relies on conditional phase shifts acquired as photons are reflected from a resonant cavity containing a single atom, which are analogous to the reflection dynamics derived for single surface plasmons here. In addition, by using surface plasmons it is possible to achieve very large optical depths with just a few emitters, which makes this system effective for realizing electromagnetically induced transparency-based nonlinear schemes[4,6–8]. Finally, the present system is an intriguing candidate to observe phenomena associated with strongly interacting, one-dimensional many-body systems. For example, non-perturbative effects such as dynamical cross-overs[42] involving photons can be explored. Higher-order correlations created in the transmitted field can become a useful tool to study and probe the non-equilibrium quantum dynamics of these strongly interacting photonic systems.

METHODS

SINGLE-PHOTON DYNAMICS

Because we are interested only in the dynamics of near-resonant photons with an emitter, we can make the approximation that left- and right-propagating photons form completely separate quantum fields[32]. We define annihilation and creation operators for the two fields, $\hat{a}_{L(R),k}, \hat{a}^{\dagger}_{L(R),k}$, where the index k runs over the range $\pm\infty$; in principle, this allows for the existence of negative-energy modes, but this is unimportant if we consider near-resonant dynamics. Under this approximation, the relevant terms in equation (1) are transformed via $\int dk \, \hbar c |k| \hat{a}^{\dagger}_k \hat{a}_k \rightarrow \int dk \, \hbar c k (\hat{a}^{\dagger}_{R,k} \hat{a}_{R,k} + \hat{a}^{\dagger}_{L,-k} \hat{a}_{L,-k})$ and $\sigma_{eg} \hat{a}_k e^{ikz_a} \rightarrow \sigma_{eg} (\hat{a}_{R,k} + \hat{a}_{L,k}) e^{ikz_a}$.

To solve for the reflection and transmission coefficients of single-photon scattering, we write the general wavefunction for a system containing one (either photonic or atomic) excitation in the following way (here, a two-level emitter is assumed),

$$|\psi_k\rangle = \int dz \left(\phi_L(z) \hat{E}^{\dagger}_L(z) + \phi_R(z) \hat{E}^{\dagger}_R(z) \right) |g, \mathrm{vac}\rangle + c_e |e, \mathrm{vac}\rangle.$$

The field amplitudes are chosen to correspond to photons of well-defined momenta in the limits $z \to \pm\infty$, for example, $\phi_R(z \to -\infty) \sim e^{ikz}$, $\phi_R(z \to \infty) \sim te^{ikz}$ and $\phi_L(z \to -\infty) \sim re^{-ikz}$ for a photon propagating initially to the right, where $t(r)$ is the transmission (reflection) coefficient. Following ref. 32, we obtain equation (2) by solving the time-independent Schrödinger equation $H|\psi_k\rangle = E_k|\psi_k\rangle$ for r, t and c_e. Here the loss term in the effective hamiltonian yields the probability that the incoming photon is lost during the scattering process, and it is not necessary to take quantum jumps into account regardless of the jump probability.

MULTIPHOTON DYNAMICS

For a coherent state input and for an emitter initialized in its ground state, the initial state can be written in the form $|\tilde{\psi}(t \to -\infty)\rangle = D(\{\alpha_k e^{-i\nu_k t}\})|\mathrm{vac}\rangle|g\rangle$, where the displacement operator $D(\{\alpha_k\}) \equiv \exp(\int \mathrm{d}k\, \hat{a}_{R,k}^\dagger \alpha_k - \alpha_k^* \hat{a}_{R,k})$ creates a multimode coherent state from vacuum[31]. This property of the displacement operator motivates a state transformation given by[43]

$$|\tilde{\psi}\rangle = D\big(\{\alpha_k e^{-i\nu_k t}\}\big)|\psi\rangle, \tag{3}$$

so that the initial state is transformed into $|\psi(t \to -\infty)\rangle = |\mathrm{vac}\rangle|g\rangle$. In the Heisenberg picture (and for a field initially propagating to the right), the right-going field operator transforms as $\hat{E}_R(z,t) \to \hat{E}_R(z,t) + \mathcal{E}_c(z,t)$, where the external field amplitude is $\mathcal{E}_c(z,t) = (1/\sqrt{2\pi})\int \mathrm{d}k\, \alpha_k e^{ikz - i\nu_k t}$. The transformation thus maps the initial coherent state to a classical Rabi frequency in the interaction hamiltonian, while simultaneously mapping the initial photonic state to vacuum. The dynamics of the emitter interacting with the field modes can now be treated under the Wigner–Weisskopf approximation, that is, interaction with the vacuum modes gives rise to an exponential decay rate from $|e\rangle$ to $|g\rangle$ at a rate Γ. The evolution of the atomic operators consequently reduces to the usual Langevin–Bloch equations[31], which enables all properties of the atomic operators and the scattered field to be calculated. Note that in these equations, the dissipative term in the effective hamiltonian of equation (1) and the quantum-jump picture is now rigorously replaced by dissipation and fluctuation (that is, noise) operators that influence evolution of the atomic operators[31].

In the two-branch approximation, the Heisenberg equations of motion for the fields are given by

$$\left(\frac{\partial}{\partial z} + \frac{1}{c}\frac{\partial}{\partial t}\right)\hat{E}_R(z,t) = \frac{\sqrt{2\pi}ig}{c}\sigma_{ge}(t)\delta(z - z_a),$$

which can be formally integrated, giving

$$\hat{E}_R(z,t) = \hat{E}_{R,\text{free}}(z - ct) + \frac{\sqrt{2\pi}ig}{c}\sigma_{ge}\left(t - (z - z_a)/c\right)\Theta(z - z_a), \tag{4}$$

where $\Theta(z)$ is the step function. A similar equation holds for $\hat{E}_L$. Assuming that the field initially propagates to the right, $\hat{E}_R(z,t)$ is the field transmitted past the emitter for $z > z_a$, whereas for $z < z_a$, $\hat{E}_L(z,t)$ is the reflected field.

Under the transformation given by equation (3), the first-order correlation function for the right-going field is given by

$$G_R^{(1)}(z,t) = \langle(\hat{E}_R^\dagger(z,t) + \mathcal{E}_c^*(z,t))(\hat{E}_R(z,t) + \mathcal{E}_c(z,t))\rangle, \tag{5}$$

which on evaluating at $z > z_a$ yields the average transmitted intensity (a similar expression holds for the reflected intensity). We proceed by substituting equation (4) into equation (5). Because the initial photonic state is vacuum following the transformation, $\hat{E}_{R,\text{free}}$ has no effect and thus calculation of $G^{(1)}$ reduces to calculating correlations between atomic operators. Techniques for evaluating these correlations are well known using the Langevin–Bloch equations[31]. Calculation of $g^{(2)}(t)$ proceeds in a similar manner by using equation (4) to express $g^{(2)}(t)$ in terms of two-time atomic correlations, which can be evaluated using the well-known quantum-regression theorem[31].

References

1. Boyd, R. W. *Nonlinear Optics* (Academic, New York, 1992).
2. Gibbs, H. M. *Optical Bistability: Controlling Light with Light* (Academic, Orlando, 1985).
3. Bouwmeester, D., Ekert, A. & Zeilinger, A. (eds) *The Physics of Quantum Information* (Springer, Berlin, 2000).
4. Schmidt, H. & Imamoglu, A. Giant Kerr nonlinearities obtained by electromagnetically induced transparency. *Opt. Lett.* **21**, 1936–1938 (1996).
5. Harris, S. E. Electromagnetically induced transparency. *Phys. Today* **50**, 36–42 (1997).
6. Harris, S. E. & Yamamoto, Y. Photon switching by quantum interference. *Phys. Rev. Lett.* **81**, 3611–3614 (1998).
7. Lukin, M. D. Colloquium: Trapping and manipulating photon states in atomic ensembles. *Rev. Mod. Phys.* **75**, 457–472 (2003).
8. Fleischhauer, M., Imamoglu, A. & Marangos, J. P. Electromagnetically induced transparency: Optics in coherent media. *Rev. Mod. Phys.* **77**, 633–673 (2005).
9. Vahala, K. (ed.) *Optical Microcavities* (World Scientific, Singapore, 2004).
10. Miller, R. *et al.* Trapped atoms in cavity QED: Coupling quantized light and matter. *J. Phys. B* **38**, S551–S565 (2005).
11. Duan, L.-M. & Kimble, H. J. Scalable photonic quantum computation through cavity-assisted interactions. *Phys. Rev. Lett.* **92**, 127902 (2004).
12. Birnbaum, K. M. *et al.* Photon blockade in an optical cavity with one trapped atom. *Nature* **436**, 87–90 (2005).
13. Waks, E. & Vuckovic, J. Dipole induced transparency in drop filter cavity-waveguide systems. *Phys. Rev. Lett.* **96**, 153601 (2006).
14. Bermel, P., Rodriguez, A., Johnson, S. G., Joannopoulos, J. D. & Soljačić, M. Single-photon all-optical switching using waveguide-cavity quantum electrodynamics. *Phys. Rev. A* **74**, 043818 (2006).
15. Chang, D. E., Sørensen, A. S., Hemmer, P. R. & Lukin, M. D. Quantum optics with surface plasmons. *Phys. Rev. Lett.* **97**, 053002 (2006).
16. Atwater, H. A. The promise of plasmonics. *Sci. Am.* **296**, 56–63 (2007).
17. Pacifici, D., Lezec, H. J. & Atwater, H. A. All-optical modulation by plasmonic excitation of CdSe quantum dots. *Nature Photon.* **1**, 402–406 (2007).
18. Maier, S. A. *Plasmonics: Fundamentals and Applications* (Springer, New York, 2006).
19. Takahara, J., Yamagishi, S., Taki, H., Morimoto, A. & Kobayashi, T. Guiding of a one-dimensional optical beam with nanometer diameter. *Opt. Lett.* **22**, 475–477 (1998).
20. Genet, C. & Ebbesen, T. W. Light in tiny holes. *Nature* **445**, 39–46 (2007).
21. Klimov, V. V., Ducloy, M. & Letokhov, V. S. A model of an apertureless scanning microscope with a prolate nanospheriod as a tip and an excited molecule as an object. *Chem. Phys. Lett.* **358**, 192–198 (2002).
22. Smolyaninov, I. I., Elliott, J., Zayats, A. V. & Davis, C. C. Far-field optical microscopy with a nanometer-scale resolution based on the in-plane image magnification by surface plasmon polaritons. *Phys. Rev. Lett.* **94**, 057401 (2005).
23. Kneipp, K. *et al.* Single molecule detection using surface-enhanced Raman scattering (SERS). *Phys. Rev. Lett.* **78**, 1667–1670 (1997).
24. Nie, S. & Emory, S. R. Probing single molecules and single nanoparticles by surface-enhanced Raman scattering. *Science* **275**, 1102–1106 (1997).
25. Kühn, S., Håkanson, U., Rogobete, L. & Sandoghdar, V. Enhancement of single-molecule fluorescence using a gold nanoparticle as an optical nanoantenna. *Phys. Rev. Lett.* **97**, 017402 (2006).
26. Bellessa, J., Bonnand, C. & Plenet, J. C. Strong coupling between surface plasmons and excitons in an organic semiconductor. *Phys. Rev. Lett.* **93**, 036404 (2004).
27. Dintinger, J., Klein, S., Bustos, F., Barnes, W. L. & Ebbesen, T. W. Strong coupling between surface plasmon-polaritons and organic molecules in subwavelength hole arrays. *Phys. Rev. B* **71**, 035424 (2005).
28. Chang, D. E., Sørensen, A. S., Hemmer, P. R. & Lukin, M. D. Strong coupling of single emitters to surface plasmons. *Phys. Rev. B* **76**, 035420 (2007).
29. Tong, L., Lou, J. & Mazur, E. Single-mode guiding properties of subwavelength-diameter silica and silicon wire waveguides. *Opt. Express* **12**, 1025–1035 (2004).
30. Nayak, K. P. *et al.* Optical nanofiber as an efficient tool for manipulating and probing atomic fluorescence. *Opt. Express* **15**, 5431–5438 (2007).
31. Meystre, P. & Sargent III, M. *Elements of Quantum Optics* 3rd edn (Springer, New York, 1999).
32. Shen, J. T. & Fan, S. Coherent photon transport from spontaneous emission in one-dimensional waveguides. *Opt. Lett.* **30**, 2001–2003 (2005).
33. Kojima, K., Hofmann, H. F., Takeuchi, S. & Sasaki, K. Nonlinear interaction of two photons with a one-dimensional atom: Spatiotemporal quantum coherence in the emitted field. *Phys. Rev. A* **68**, 013803 (2003).
34. Shen, J.-T. & Fan, S. Strongly correlated two-photon transport in a one-dimensional waveguide coupled to a two-level system. *Phys. Rev. Lett.* **98**, 153003 (2007).
35. Carmichael, H. J., Brecha, R. J. & Rice, P. R. Quantum interference and collapse of the wavefunction in cavity QED. *Opt. Commun.* **82**, 73–79 (1991).
36. Cirac, J. I., Zoller, P., Kimble, H. J. & Mabuchi, M. Quantum state transfer and entanglement distribution among distant nodes in a quantum network. *Phys. Rev. Lett.* **78**, 3221–3224 (1997).
37. Gorshkov, A. V., Andre, A., Fleischhauer, M., Sørensen, A. S. & Lukin, M. D. Universal approach to optimal photon storage in atomic media. *Phys. Rev. Lett.* **98**, 123601 (2007).
38. Fleischhauer, M. & Lukin, M. D. Dark-state polaritons in electromagnetically induced transparency. *Phys. Rev. Lett.* **84**, 5094–5097 (2000).
39. Maier, S. A., Friedman, M. D., Barclay, P. E. & Painter, O. Experimental demonstration of fiber-accessible metal nanoparticle plasmon waveguides for planar energy guiding and sensing. *Appl. Phys. Lett.* **86**, 071103 (2005).
40. Klimov, V. I. *et al.* Optical gain and stimulated emission in nanocrystal quantum dots. *Science* **290**, 314–317 (2000).
41. Brouri, R., Beveratos, A., Poizat, J.-P. & Grangier, P. Photon antibunching in the fluorescence of individual color centers in diamond. *Opt. Lett.* **25**, 1294–1296 (2000).
42. Lesage, F. & Saleur, H. Boundary interaction changing operators and dynamical correlations in quantum impurity problems. *Phys. Rev. Lett.* **80**, 4370–4373 (1998).
43. Mollow, B. R. Pure-state analysis of resonant light scattering: Radiative damping, saturation, and multiphoton effects. *Phys. Rev. A* **12**, 1919–1943 (1975).